Metal–Organic Frameworks

DOI: 10.1002/anie.201204573

Spectroscopic Evidence for the Structure Directing Role of the Solvent in the Synthesis of Two Iron Carboxylates**

*Tadeja Birsa Čelič, Mojca Rangus, Károly Lázár, Venčeslav Kaučič, and Nataša Zabukovec Logar**

Metal-organic framework materials (MOFs) are crystalline solids that have inorganic building units covalently bonded to organic molecules, typically polycarboxylates, to form three-dimensional structures with different porosities.[1] The ability to precisely design the structure of MOFs for specific applications, such as for gas storage and separation, catalysis, drug delivery, and batteries, is considered to be one of their most important advantages. Some general principles for controlling the formation of targeted MOFs have been established by simply correlating their crystal structures and synthesis conditions during classical or high-throughput syntheses.[2] Very few studies have gone further by also highlighting the formation mechanism and detecting the fundamental building blocks of growth and/or intermediate phases because such investigations appear to be a great experimental challenge.[2,3]

Currently, detailed studies of the solution species before the MOFs crystallize have been performed using X-ray absorption spectroscopy (XAS),[4a] mass spectrometry,[4b] energy-dispersive X-ray diffraction,[4c,d,e] X-ray scattering (SAXS/WAXS),[4f,g] and NMR spectroscopy.[4h] The results from these studies confirmed the formation of secondary building units and explained the roles of the type of metal and organic linker as well as the heating regime on the crystallization kinetics. Only one study has focused on the role of the solvent,[4f] although reaction media have been reported to have a profound impact on the formation of the framework.[5,6] The results indicated that the solubility of the ligand significantly affected the crystallization kinetics.[4f] However, no information on the type of building units that assemble during crystallization were provided; therefore, possible effects, such as the ability of the solvent to act as a ligand, could not be properly considered. The authors emphasized the need to use XAS or vibrational spectroscopies,[7] to complement X-ray scattering experiments.

Here, we report a detailed Fe K-edge XAS and Mössbauer spectroscopy study on the role of the type and composition of solvent on the competitive formation of the MIL-100(Fe) and MIL-45(Fe) structures. It is the second XAS study of MOF formation, and the first study that evaluates the role of the solvent in the formation process by analyzing the local structure of the species that are present in the precursor solution and gel. The two investigated materials were prepared from the same metal and organic precursors by changing a single synthesis parameter—the solvent composition (H_2O or H_2O/acetone), while all other variables (time, temperature, and molar ratios) were kept constant (Table S1 in the Supporting Information). The two studied structures differ in the connectivity of the metal building units and organic linkers and in the oxidation states of the iron ion (Figure 1). Because ferric chloride was used as the iron source for both structures, and the iron in MIL-45(Fe) is divalent, the $Fe^{III} \rightarrow Fe^{II}$ reduction must have occurred sometime during the synthesis of this material. The stage at which this change occurs was ambiguously determined in the present study.

During the XAS investigation, we first focused on the dissolution of the iron source ($FeCl_3 \cdot 6H_2O$) in a solvent, which was water or a mixture of water and acetone. The samples are denoted as MIL-100(Fe)-S and MIL-45(Fe)-S,

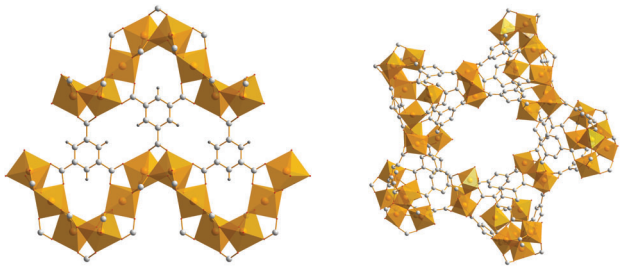

Figure 1. Structures of MIL-45(Fe) (left) and MIL-100(Fe) (right). The pure iron analogue of MIL-45[8] consists of chains of iron(II) octahedra that are linked through benzene-1,3,5-tricarboxylic (BTC) anions to form a three-dimensional framework. The two crystallographically distinct iron sites in MIL-45(Fe) are both six-coordinated to oxygen atoms from trimesate. The more known MIL-100(Fe)[9] is formed from trimers of μ_3-O-bridged iron(III) octahedra (seven crystallographically distinct sites), which are connected by BTC linkers into a large-pore framework structure.

[*] T. Birsa Čelič, Dr. M. Rangus, Prof. V. Kaučič, Prof. N. Zabukovec Logar
Laboratory for Inorganic Chemistry and Technology
National Institute of Chemistry
Hajdrihova 19, 1000 Ljubljana (Slovenia)
and
Centre of Excellence Low Carbon Technologies
Hajdrihova 19, 1000 Ljubljana (Slovenia)
E-mail: natasa.zabukovec@ki.si
Dr. K. Lázár
Centre for Energy Research, Institute of Isotopes, HAS
P.O. Box 77, 1525 Budapest (Hungary)

[**] This work was supported by the Slovenian Research Agency research programme P1-0021, Sloveninan-Hungarian bilateral project TÉT_10-1-2011-0624, DESY, and the EU FP7/2007-2013 programme ELISA (grant number 226716). Access to SR facilities of ELETTRA (project number 20105073) and HASYLAB (project II-20080058 EC), and collaboration with Prof. Iztok Arčon is acknowledged.

Supporting information for this article is available on the WWW under http://dx.doi.org/10.1002/anie.201204573.

respectively. The molar ratios of ferric chloride to solvent were kept constant throughout the study. In the Fe K-edge XANES spectra (Figure 2), the energy positions of the adsorption edges revealed that in both cases the oxidation

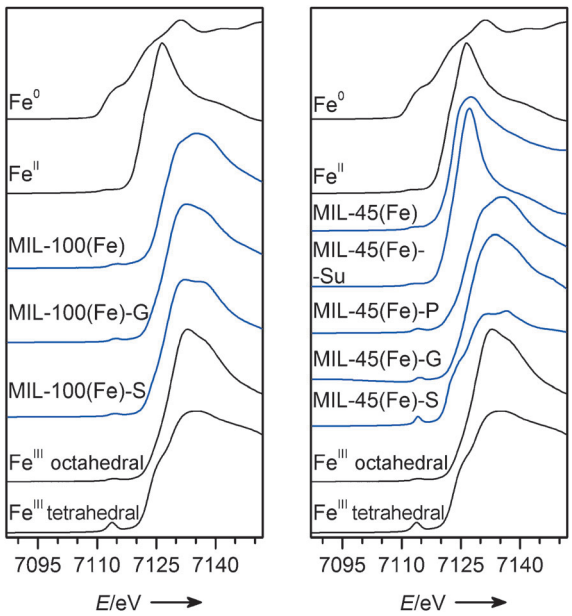

Figure 2. Normalized Fe K-edge XANES spectra of selected solutions, gels, and final crystalline samples of MIL-100(Fe) (left) and MIL-45(Fe) (right) along with references compounds (Fe metal–Fe^0, $FeSO_4 \cdot 7H_2O$–Fe^{II}, $Fe_2(SO_4)_3 \cdot 5H_2O$–Fe^{III} octahedral and $FePO_4 \cdot 2H_2O$–Fe^{III} tetrahedral). The spectra are displaced vertically for clarity. In the case of MIL-45(Fe), the stage in the synthesis where the iron is reduced manifests as a shift of the absorption edge towards lower energies.

state of iron is 3+ (Table S4). Furthermore, the shape and intensity of the pre-edge feature indicated that the Fe ions are in an octahedral coordination in MIL-100(Fe)-S and in tetrahedral or a combination of tetrahedral and octahedral coordinations in MIL-45(Fe)-S. The analysis of the EXAFS region of the XAS spectra (Figure 3) revealed that in MIL-100(Fe)-S the iron atom is coordinated to four water molecules and two chlorine atoms, which is the same as in the $FeCl_3 \cdot 6H_2O$ crystal structure (Table 1) and from which it can be concluded that iron chloride did not completely dissolve because of the high $FeCl_3 \cdot 6H_2O$ to water molar ratio (1:29). In MIL-45(Fe)-S 75% of iron atoms are four-fold coordinated to Cl ions forming $[FeCl_4]^-$ complexes and 25% of iron is octahedrally coordinated with six O atoms from water molecules (see the Supporting Information). The analysis gave no evidences of the presence of dinuclear and trinuclear iron oxohydroxochlorido complexes that are common hydrolysis products of $FeCl_3 \cdot 6H_2O$ in water[10] in neither of the two samples.

The second step was an investigation of the prepared reaction gels (denoted as MIL-100(Fe)-G and MIL-45(Fe)-G) before they were placed into Teflon-lined autoclaves. A XANES study indicated that iron has an octahedral coordination and remains in a trivalent form in both reaction gels. An EXAFS analysis confirmed that the Fe ions are coordi-

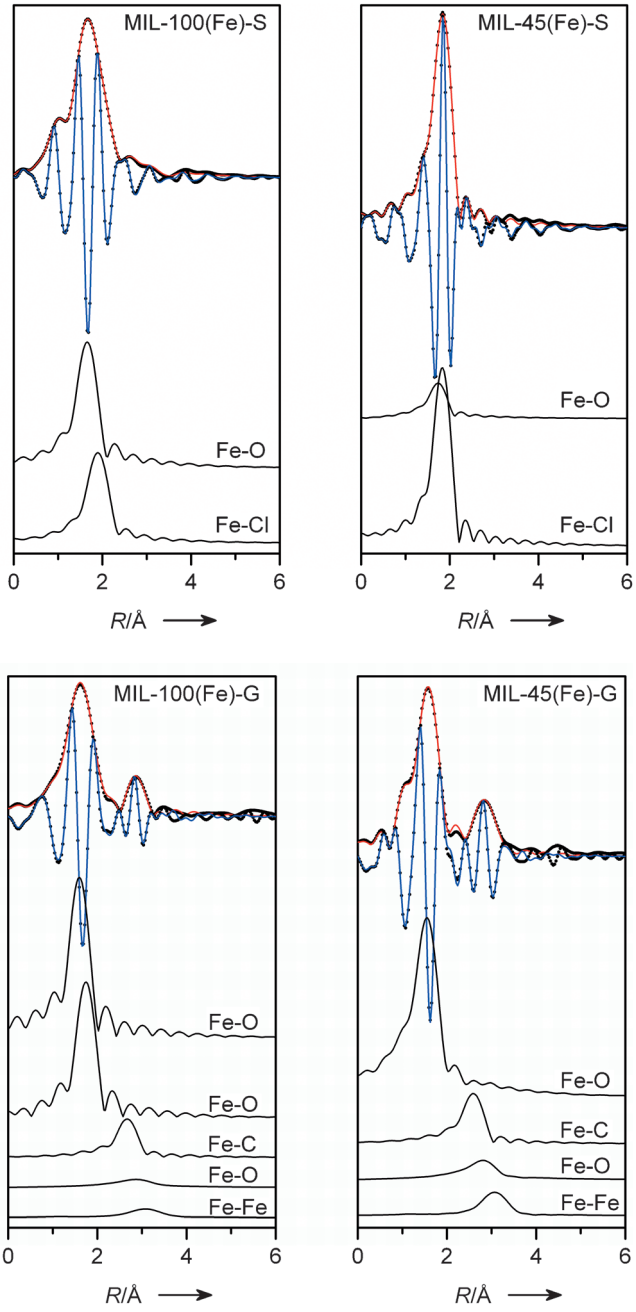

Figure 3. The k^3-weighed Fourier transformed Fe K-edge EXAFS spectra of selected solutions (upper part of the figure) and gels (lower part of the figure). Experimental data (black dots) are presented along with best fit of the FT magnitude (red line) and imaginary part (blue line). Individual single scattering paths (black lines) are also shown.

nated by six oxygen atoms (Table 1) and also revealed the presence of C atoms at distances of approximately 3.0 Å for both initial gels. This result suggests that the trimesic acid is already connected to the iron ions at this stage in the synthesis. In addition, the best fit indicated two iron atoms in the second coordination shell, which means that the Fe atoms form larger complexes or precursors that have well-defined structures. These precursors could have iron ions connected with BTC linkers forming chains (similar as in the final MIL-

Table 1: Refined EXAFS structural parameters of the first and second coordination shell around Fe atoms; type of neighboring atom, average number *N*, distance *R*, and Debye–Waller factor, σ^2.[a]

Sample	Neighbor type	*N*	*R* [Å]	σ^2 [Å^2]
MIL-100(Fe)-S	O	4	2.027(2)	0.0049(2)
	Cl	2	2.283(2)	0.0069(3)
	H	8	2.69(2)	0.009(2)
MIL-45(Fe)-S	25% O	6	2.01(1)	0.0046(7)
	75% Cl	4	2.213(4)	0.0040(2)
MIL-45(Fe)-G	O	6	1.993(3)	0.0091(4)
	C	5.33	3.04(1)	0.006(2)
	O	4(2)	3.30(6)	0.016(5)
	Fe	2	3.47(3)	0.016(5)
MIL-100(Fe)-G	O	3	1.994(4)	0.002(1)
	O	3	2.139(5)	0.002(1)
	C	4	3.09(1)	0.004(1)
	Fe	2	3.45(9)	0.025(4)
MIL-45(Fe)-Su	O	4	3.4(1)	0.025(4)
	O	5.8(2)	2.116(2)	0.0076(3)
	O	6	2.028(6)	0.008(1)
MIL-45(Fe)-P	C	5	3.01(2)	0.008(3)
	O	3(2)	3.32(8)	0.008(3)
	Fe	0.9(7)	3.39(6)	0.008(3)

[a] For the following samples: MIL-100(Fe)-S (Δk = 5.0–12.5 Å^{-1}; ΔR = 1.0–4.5 Å), MIL-45(Fe)-S (Δk = 4.0–14.0 Å^{-1}; ΔR = 1.0–2.5 Å), MIL-100(Fe)-G (Δk = 3.8–11.5 Å^{-1}; ΔR = 1.0–3.5 Å), MIL-45(Fe)-G (Δk = 3.8–11.5 Å^{-1}; ΔR = 1.0–3.6 Å), MIL-45(Fe)-Su (Δk = 3.0–12.5 Å^{-1}; ΔR = 1.0–3.0 Å), and MIL-45(Fe)-P (Δk = 3.9–11.5 Å^{-1}; ΔR = 1.0–3.4 Å). Uncertainties in the last digit are given in parentheses.

45 structure) or iron trimers (such as in the final MIL-100 structure, Figure 3). The existence of separated iron trimeric clusters was already proposed in the EXAFS study on the formation of MIL-89.[4a] In our case, however it was not possible to discriminate between the two possible precursors because of the similar interatomic distances of the separated trimer in MIL-100(Fe) and a trimer fragment from the chain structure of MIL-45(Fe) (Figure 1) as well as because of a large overlap of the contributions in the second coordination shell of Fe atoms.

From the results obtained thus far, it is obvious that during the MIL-45(Fe) synthesis, the change in the iron oxidation state from 3+ to 2+ does not occur before the thermal treatment in auctoclaves. To explain this phenomenon, the crystallization was stopped after 8 h and the contents of the autoclave were examined. The sample consisted of a precipitate (MIL-45(Fe)-P) at the bottom of the vessel and a liquid supernatant (MIL-45(Fe)-Su) at the top. The XANES spectrum of the supernatant exhibits a significant shift of the Fe K absorption edge towards lower energies compared to the edge position of MIL-45 initial gel (Figure 2), which indicates that the iron in the liquid phase has been reduced to Fe^{II}. We would also expect that while the oxidation number of iron has changed, the majority of the Fe–O bonds (bonds between iron and carboxylic oxygen atoms) would break. The EXAFS analysis confirmed this assumption (Table 1 and Figure S12). The Fe atoms in the supernatant are octahedrally coordinated to six water molecules. We also observed no evidence of C atoms in the second coordination sphere indicating that the Fe atoms in the supernatant are not coordinated to BTC molecules at this stage in the synthesis. In the precipitate on the bottom of the autoclave (MIL-45(Fe)-P), the Fe ions remained in the 3+ valence state and, similarly as in the gel, C atoms were observed in the second coordination shell, which indicates that Fe atoms are still coordinated to the BTC linkers. The best fit also gave less than two Fe atoms at the approximate distance of 3.38 Å, which supports the proposed decomposition of iron complex in the precipitate when the iron is reduced to the oxidation state 2+.

The oxidation state of the Fe atoms in the final materials MIL-45(Fe) and MIL-100(Fe) was also examined using XAS analysis. The shapes and energy positions of the edge and the pre-edge resonances of the final MIL-45(Fe) sample are characteristic for octahedrally coordinated Fe^{II} cations, which is in agreement with the XRD results (see Figure S6 in the Supporting Information). The XANES study of the final MIL-100(Fe) revealed that iron is in trivalent form and octahedrally coordinated, which is the same as in the iron analogue with fluorine atoms (see Figure 4).[9]

For a more thorough investigation of the reduction of iron during the synthesis of MIL-45(Fe), the initial gel and autoclave contents were also investigated using Mössbauer spectroscopy (Figure 5). The spectrum of initial gel, MIL-45(Fe)-G, corresponds to two Fe^{III} sites in the structure with isomer shift, IS, values 0.48 and 0.50, and quadrupole splittings, QS, 0.30 and 0.81 mm s^{-1}, respectively. The examination of the supernatant that formed after one hour of thermal treatment (MIL-45(Fe)-Su-1h) indicated that all of the iron in the solution is reduced to Fe^{II}. In the MIL-45(Fe)-P-1h, the sample spectrum still resembles the MIL-45(Fe)-G spectrum, although a new Fe^{II} component appears (IS 1.37 and QS 3.29 mm s^{-1}).

Therefore, the Mössbauer spectra confirm the completion of the $Fe^{III} \rightarrow Fe^{II}$ reduction at a very early stage of the thermal treatment. With the increasing time of the thermal treatment, the amount of iron in the supernatant slowly increased as its amount in the precipitate decreased, which was confirmed by EDX elemental analysis of dried precipitate samples at different stages of treatment (see the Supporting Information). At a later stage of the synthesis, the MIL-45(Fe) crystals containing Fe^{II} ions were formed from the liquid phase. In accordance with XAS analysis of the final products, the Mössbauer spectra also prove the exclusive presence of Fe^{III} in MIL-100(Fe) and Fe^{II} in MIL-45(Fe) (Table S5). The described reduction of iron is accompanied by the formation of acetic acid as an oxidation product. It was determined in the solution next to the final MIL-45(Fe) product by gas chromatography [(1.9 ± 0.1) mg mL^{-1}].

In summary, this study provides relevant new insights into the formation of MOFs and adds to better optimization of targeted syntheses of MOFs. We have shown that in the

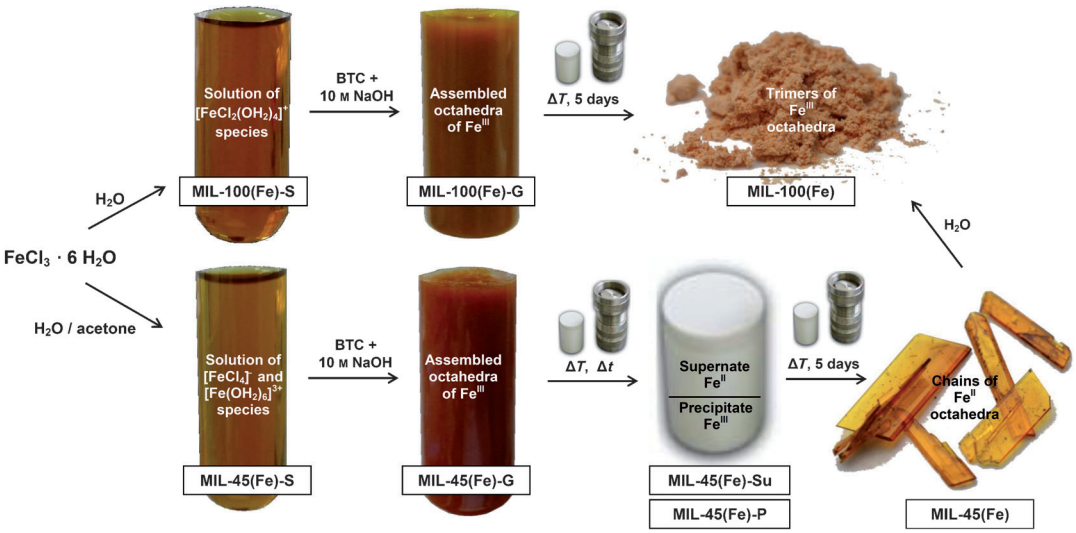

Figure 4. Schematic presentation of the crystallization process of MIL-100(Fe) and MIL-45(Fe) in different solvents determined by XAS/Mössbauer study.

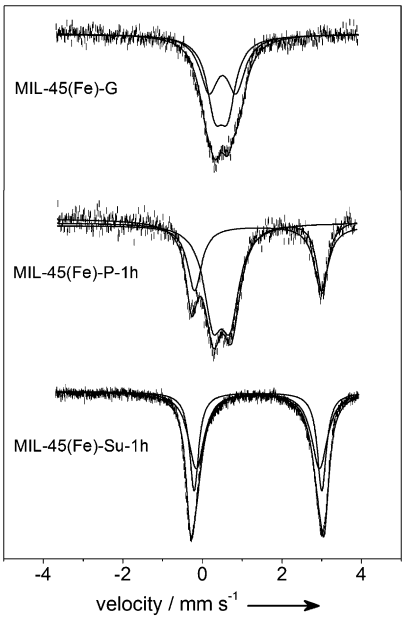

Figure 5. 77 K Mössbauer spectra of MIL-45(Fe) initial gel and intermediate products of the solvothermal synthesis.

formation process of porous iron carboxylates, acetone as a solvent can have a reductive and consequently a structure-directing role at higher temperatures. In our particular case, the presence of acetone resulted in the change of the iron oxidation state from 3+ to 2+ and the dissolution of the previously formed amorphous iron complex in the gel. The aggregation of the resulting hexa-aquo Fe^{II} species and BTC ligands enables crystallization of MIL-45(Fe) structure. In the absence of acetone the amorphous trinuclear Fe^{III} complexes in the gel condensate further into the MIL-100(Fe) framework.

We have also shown that the aprotic acetone influences the rate of the solvation process of the reagents by evidencing the differences in the speciation of iron in the examined solutions and gels. However, the exact reactions that occur in the very concentrated systems could only be anticipated. In both cases the absence of polynuclear hydrolysis products of iron in the starting solutions suggests a one-step complexation of iron mononuclear species and BTC linkers into characteristic complexes found in the gels: trimeric complex in MIL-100 system and short chains in MIL-45 system. The formation of trimeric Al complexes was also determined by in situ NMR study of MIL-100(Al) crystallization, which was published after the present manuscript was submitted.[4h] As already stated by the authors, a slightly different complexation path (dimeric Al_2-BTC_2, formed first, later reacts with hexa-aquo Al^{III} complex) is expected because of the quite different solution chemistry of Al^{III} and Fe^{III} or Cr^{III} ions.

When checking the hydrothermal stability of MIL-45(Fe) and MIL-100(Fe) products, precisely when the crystals of the final MIL-45(Fe) were placed into water for 16 h, an irreversible solid–solid transformation to MIL-100(Fe) occurred (see Figure S8 in the Supporting Information). The results suggest that MIL-45(Fe) is a metastable phase that eventually evolves into the thermodynamically more stable MIL-100(Fe) structure. A similar transformation phenomenum was observed in the NH_2-MIL-101(Al)/NH_2-MIL-53(Al) system.[4f]

Experimental Section

The X-ray absorption spectra of the analyzed materials and the reference compounds were measured in the Fe K-edge energy region (7112 eV) in the transmission detection mode at the XAFS beamline of the ELETTRA synchrotron facility in Basovizza, Italy and at the A1 beamline at the HASYLAB synchrotron facility at DESY in Hamburg, Germany. The Mössbauer spectra were recorded on a KFKI spectrometer in constant acceleration mode (see the Supporting Information).

Received: June 12, 2012
Revised: October 17, 2012
Published online: November 13, 2012

Keywords: crystallization · EXFAS spectroscopy · metal–organic frameworks · Moessbauer spectroscopy

[1] G. Férey, *Chem. Soc. Rev.* **2008**, *37*, 191 – 214.
[2] N. Stock, S. Biswas, *Chem. Rev.* **2012**, *112*, 933 – 969.
[3] N. Pienack, W. Bensch, *Angew. Chem.* **2011**, *123*, 2062 – 2083; *Angew. Chem. Int. Ed.* **2011**, *50*, 2014 – 2034.
[4] a) S. Surblé, F. Millange, C. Serre, G. Férey, R. I. Walton, *Chem. Commun.* **2006**, 1518 – 1520; b) J. A. Rood, W. C. Boggess, B. C. Noll, K. W. Henderson, *J. Am. Chem. Soc.* **2007**, *129*, 13675 – 13682; c) F. Millange, I. M. Medina, N. Guillou, G. Férey, K. M. Golden, R. I. Walton, *Angew. Chem.* **2010**, *122*, 775 – 778; *Angew. Chem. Int. Ed.* **2010**, *49*, 763 – 766; d) F. Millange, R. El Osta, M. E. Medina, R. I. Walton, *CrystEngComm* **2011**, *13*, 103 – 108; e) T. Ahnfeldt, J. Moellmer, V. Guillerm, R. Staudt, C. Serre, N. Stock, *Chem. Eur. J.* **2011**, *17*, 6462 – 6468; f) E. Stavitski, M. Goesten, J. Juan-Alcañiz, A. Martinez-Joaristi, P. Serra-Crespo, A. V. Petukhov, J. Gascon, F. Kapteijn, *Angew. Chem.* **2011**, *123*, 9798 – 9802; *Angew. Chem. Int. Ed.* **2011**, *50*, 9624 – 9628; g) J. Juan-Alcañiz, M. Goesten, A. Martinez-Joaristi, E. Stavitski, A. V. Petukhov, J. Gascon, F. Kapteijn, *Chem. Commun.* **2011**, *47*, 8578 – 8580; h) M. Haouas, C. Volkringer, T. Loiseau, G. Férey, F. Taulelle, *Chem. Mater.* **2012**, *24*, 2462 – 2471.
[5] C.-P. Li, M. Du, *Chem. Commun.* **2011**, *47*, 5958 – 5972.
[6] a) P. M. Forster, N. Stock, A. K. Cheetham, *Angew. Chem.* **2005**, *117*, 7780 – 7784; *Angew. Chem. Int. Ed.* **2005**, *44*, 7608 – 7611; b) D. M. Shin, I. S. Lee, D. Cho, Y. K. Chung, *Inorg. Chem. Commun.* **2003**, *6*, 7722 – 7724; c) B.-C. Tzeng, H.-T. Yeh, T.-Y. Chang, G.-H. Lee, *Cryst. Growth Des.* **2009**, *9*, 2552 – 2555; d) C.-P. Li, Y.-L. Tian, Y.-M. Guo, *Inorg. Chem. Commun.* **2008**, *11*, 1405 – 1408; e) A.-Y. Fu, Y.-L. Jiang, Y.-Y. Wang, X.-N. Gao, G.-P. Yang, L. Hou, Q.-Z. Shi, *Inorg. Chem.* **2010**, *49*, 5495 – 5502; f) E. Tynan, P. Jensen, P. E. Kruger, A. C. Lees, *Chem. Commun.* **2004**, 776 – 777; g) F.-K. Wang, S.-Y. Yang, R.-B. Huang, L.-S. Zheng, S. R. Batten, *CrystEngComm* **2008**, *10*, 1211 – 1215; h) R. Peng, S.-R. Deng, M. Li, D. Li, Z.-Y. Li, *CrystEngComm* **2008**, *10*, 590 – 597; i) Y.-Y. Yang, W. Guo, M. Du, *Inorg. Chem. Commun.* **2010**, *13*, 1195 – 1198.
[7] a) S. Gross, M. Bauer, *Adv. Funct. Mater.* **2010**, *20*, 4026 – 4047; b) S. Bordiga, F. Bonino, K. P. Lillerud, C. Lamberti, *Chem. Soc. Rev.* **2010**, *39*, 4885 – 4927.
[8] M. Riou-Cavellec, C. Albinet, C. Livage, N. Guillou, A. Noguès, J.-M. Grenèche, G. Férey, *Solid State Sci.* **2002**, *4*, 267 – 270.
[9] P. Horcajada, S. Surblé, C. Serre, D.-Y. Hong, Y.-K. Seo, J.-S. Chang, J.-M. Grenèche, I. Margiolaki, G. Férey, *Chem. Commun.* **2007**, 2820 – 2822.
[10] H. Hellman, R. S. Laitinen, L. Kaila, J. Jalonen, V. Hietapelto, J. Jokela, A. Sarpola, J. Rämö, *J. Mass Spectrom.* **2006**, *41*, 1421 – 1429.

